Title: Influence of lanthanum dopant on the structure and electric properties of BaBi2Nb2O9 ceramics

Author: Małgorzata Adamczyk-Habrajska, Tomasz Goryczka, Diana Szalbot, Jolanta Dzik, Michał Rerak, Dariusz Bochenek
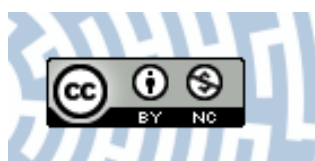
UNIWERSYTET ŚLĄSKI W KATOWICACH

Biblioteka Uniwersytetu Śląskiego

Ministerstwo Nauki i Szkolnictwa Wyższego

M. ADAMCZYK-HABRAJSKA[1]*, T. GORYCZKA[1], D. SZALBOT[1],
J. DZIK[1], M. RERAK[1], D. BOCHENEK[1]

INFLUENCE OF LANTHANUM DOPANT ON THE STRUCTURE AND ELECTRIC PROPERTIES
OF BaBi$_2$Nb$_2$O$_9$ CERAMICS

The paper reports the consequences of lanthanum modifications of barium bismuth niobiate (BaBi$_2$Nb$_2$O$_9$) ceramics. The discussed materials were prepared by solid state synthesis and a one-step sintering process. The investigations are focused on dielectric aspects of the modification. The presented results reveal that the trivalent lanthanum ions incorporate twovalent barium ions, which is connected with the creation of A-site cationic vacancies as well as oxygen vacancies. Such a scenario results in significant decreasing in grain boundaries resistivity. The activation energy of grain boundaries conductivity is significantly reduced in the case of lanthanum admixture.

Keywords: Ferroelectric relaxor, Ceramics, Impedance spectroscopy

1. Introduction

BaBi$_2$Nb$_2$O$_9$ (BBN) belongs to one of the three types of layered perovskites, namely Aurivillius phases. The crystallographic structure of this compound is complex and can be described by the general formula of $(Bi_2O_2)^{2+}(A_{n-1}B_nO_{2n+1})^{2-}$, where $(A_{n-1}B_nO_{2n+1})^{2-}$ represents the perovskite-like blocks between $(Bi_2O_2)^{2+}$ slabs. Such convoluted crystal structure is the starting point to very interesting, although difficult to interpret, properties [1-6]. Based on the analysis of the valence of the atom in the A sub-lattice, the discussed type of compounds can be divided into two groups. The first one, exemplified by Bi$_4$Ti$_3$O$_{12}$ or Bi$_3$TiNbO$_3$ [6-8], includes structures characterized by too low valence of ions in A sub-lattice. The second group are the structures in which A cations have inflated valence. A standard example of such materials are the ceramics discussed in the paper.

The complexity of the crystal structure of the discussed BBN ceramics leads to the complicated dynamics of the crystal lattice. The dynamics consist of:
- oscillation along polar axis (a) of crystal lattice,
- rotation around (a) and (c) axes of crystal lattice.

The BBN ceramics show features characteristic of ferroelectric relaxors (FR), namely the strong frequency dependences of the maximum value of dielectric permittivity and the shifts of its maximum to high temperatures, with an increase of frequency. The second feature typical for FR observed in BBN ceramics is the strong deviation from the Curie-Weiss law in wide ranges of temperatures, above the temperature of maximum permittivity (T_m). Moreover, in FR, as opposed to classic ferroelectric materials, the maximum of dielectric permittivity is not related to the structural phase transition, which has been confirmed by temperature XRD measurements [9-11]. Also, this feature is characteristic of BBN ceramics – the temperature dependences of lattice parameter, measured during heating, does not reveal the existence of a structural phase transition, but the growth of the parameters connected with the classic thermal expansion, only. However, a more thorough analysis of the temperature dependences of lattice parameters (particularly $c(T)$) reveals that the increase is not linear – which was widely discussed in paper [12]. The results presented in the aforementioned paper confirmed the conclusion made by Y. Shimakawa [13], who postulated that the macroscopic tetragonal structure of BBN ceramics (with the following space group I4mm [14]) contains microregions characterized by orthorhombic distortion, the appearance of which is the result of the chemical inhomogeneity. The distortion in the discussed regions disappeared with a gradual increase of temperature – the symmetry in microregions changes from orthorhombic to tetragonal.

[1] UNIVERSITY OF SILESIA, FACULTY OF SCIENCE AND TECHNOLOGY, INSTITUTE OF MATERIALS ENGINEERING, 12, ZYTNIA STR., 41-200 SOSNOWIEC, POLAND

* Corresponding author: malgorzata.adamczyk-habrajska@us.edu.pl

The discussed material has a common interesting feature which is crucial for the investigations described in the paper. Namely, worldwide literature reports the effect of shrinking lack – the replacement of barium, strontium or niobium ions by the ones possessing significantly smaller ionic radius, should be reflected by a gradual reduction of crystal lattice parameters [15-17]. However, the author of papers [18,19] reports that for the lower contents of dopants, the crystal parameters remain unchanged. The changes are observed only after crossing a certain threshold of the dopant concentration. The authors of the paper claim that $(Bi_2O_2)^{2+}$ layers are responsible for such behavior. The layers prevent the structure from shrinking. The influence of the layer is limited, of course. After exceeding a certain value, the stress of the structure is so high that the shrinking process is activated. In summary, small amount of dopant with a small value of ionic radius creates a lot of free space in the crystal structure and influence on dielectric properties.

The present paper describes the results of dielectric and impedance measurement of lanthanum modified $BaBi_2Nb_2O_9$ ceramics. The literature reports that trivalent lanthanum ions incorporate twovalent barium ions, which causes the creation of A-site cationic vacancies. The defect reaction has the following formula [20]:

$$La_2O_3 \rightarrow 2La_{Ba}{}^* + 3O_o{}^x + V_{Ba}{}''$$
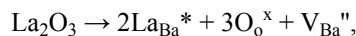
where $La_{Ba}{}^*$ represents a lanthanum ion in the barium site with one effective positive charge, $O_o{}^x$ represents an oxygen ion in the oxygen site without any effective charge, and $V_{Ba}{}''$ represents barium vacancies with two effective negative charges. Such a scenario destructs chemical homogeneity on the A site and causes changes in electric and dielectric properties. The second scenario assumes the competitive way of the incorporation of lanthanum ions – with an increase of admixture concentration increase of lanthanum ions number replaced Bi^{3+} ones as a homovalent modifier. The possibility is described in literature [21,22]. The aim of the paper is to decide which one is more likely.

2. Materials and method characterization

The pure and lanthanum modified $BaBi_2Nb_2O_9$ ceramics were prepared using the conventional mixed-oxide processing technique, starting from the stoichiometric amounts of $BaCO_3$ (99.9%, Aldrich), Bi_2O_3 (99.9%, Aldrich), La_2O_5 (99.9%, Aldrich) and Nb_2O_5 (99.9%, Aldrich) reagents. Stoichiometric amounts of ceramic powders were weighed and mixed in a planetary mill (Fritsch, Pulverisette 6) in ethyl alcohol for 24 h and next were dried. Then the mixed powders were pressed into pellets. The two-step technological processes were applied to all studied ceramic materials. The condition of the first step (synthesis) was the following: temperature – 1223 K and time – 2 h. After this, the ceramic powders were crushed, milled and sieved and next pressed again into pellets. The second step of technological processes (sintering) was used to prepare ceramic materials with a well-formed microstructure. The samples were

sintered in closed crucibles at 1373 K for base BBN material and at 1423 K for lanthanum modified ones. The time of sintering was equal to 6 h. After sintering the samples were grounded, polished, annealed and the silver paste electrodes have been put on both of their surfaces (without thermal treatment).

The density of obtained ceramic samples was evaluated by using the Archimedes method, whereas the microstructure was examined by a scanning electron microscope (SEM), JSM-7100F
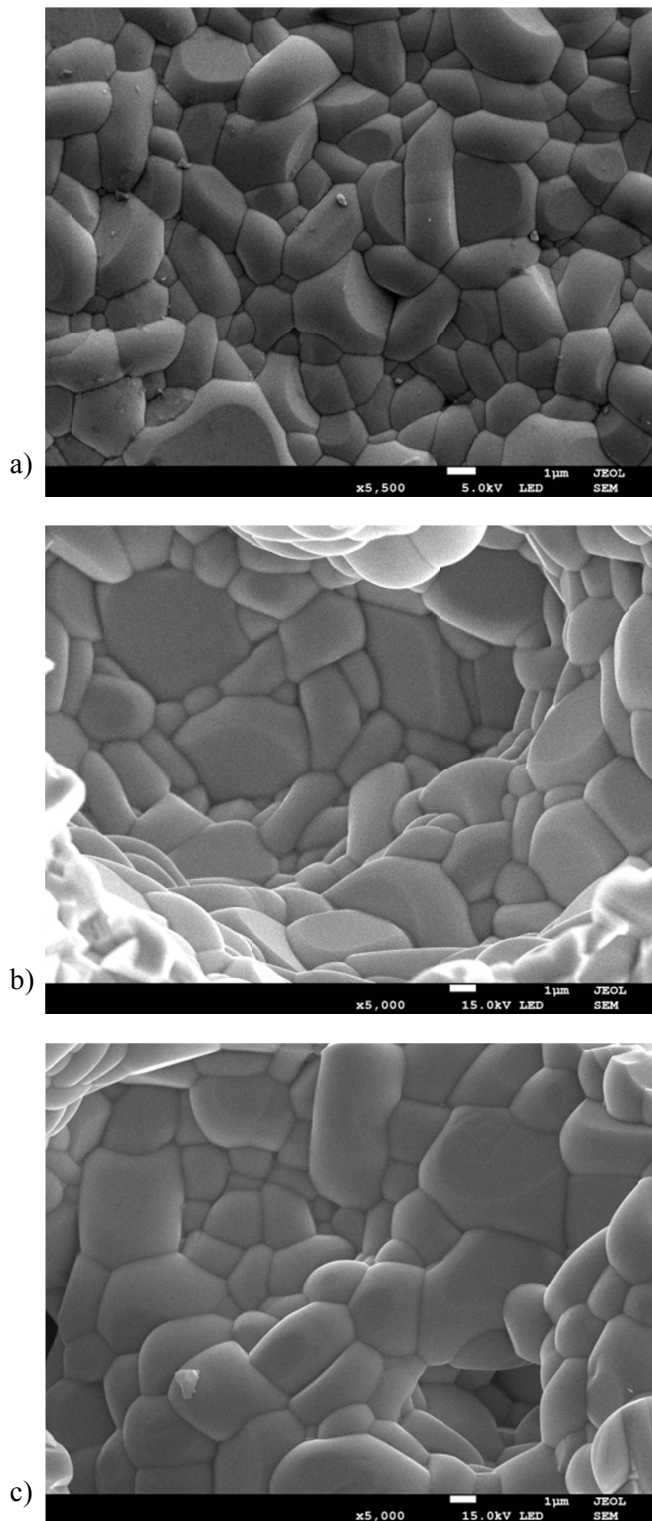

Fig. 1. SEM pictures of $BaBi_2Nb_2O_9$ ceramics a) without doping b) doped with 1 at. % La c) doped with 5 at. % La

TTL LV. The measurements were performed on the fractured surface of ceramics. The crystal structure of the discussed materials was studied using the X-ray diffraction technique (XRD). Measurements were carried out at room temperature with use of X'Pert Pro diffractometer equipped with Cu Kα_{1and2} radiation (40 kV, 30 mA).

The samples of the thickness of 0.6 mm were cut and polished for $\varepsilon(T)$ and impedance spectroscopy (IS). Subsequently, gold electrodes were deposited on them by cathode sputtering. Consecutively, the samples were deaged by thermal treatment at 723 K, prior to measurements, to allow the recombination and relaxation of part of the frozen defects, formed during the sintering process. The dielectric data, as well as impedance, were obtained in the 20 Hz-2 MHz frequency range, using an impedance analyzer. The temperature range was followed 673 K-823 K. The coherence of the obtained data was performed by K-K validation test [23,24]. Data fitting was carried out using the ZView equivalent circuit software produced by Scribner Associates.

3. Results and discussion

The microstructure of the investigated ceramics is shown in Fig. 1.

The grains as well as grains boundaries of the investigated ceramics are well developed and have plate-like shape with rounded corners. The shape is a consequence of the high grain growth in the direction perpendicular to the c-axis and the reason of anisotropic nature of Aurivillius materials crystal structure [25,26].The lanthanum dopant causes increasing in inhomogeneity of grain size, however the small grains predominate. The relative density obtained by the Archimedes method with distilled water is practically unchanged – for unmodified ceramics is equal to 7.07 g/cm^3, whereas the relative density of ceramics modified by 5 at.% of lanthanum is equal to 7.09 g/cm^3.

The crystal structure of discussed ceramics was characterized by powder X-ray diffraction. Crystallographic structure was refined using the Rietveld method. Results are shown in Fig. 2.

The pattern of pure BBN ceramics was widely described in our previous paper [27]. All detected peaks belonged to the tetragonal Aurivillius type structure. Lattice parameters calculated from refinement are compared in Table 1. The detailed analysis of obtained results point at the homogeneity of obtained structure.

TABLE 1

The lattice parameters of calcium doped BaBi$_2$Nb$_2$O$_9$ ceramics

x at.% La^{3+}	a [A]	b [A]	c [A]	V [A^3]
0	3.9406	3.9406	25.6378	398.1
1	3.9297	3.9297	25.6174	395.6
5	3.9335	3.9335	25.6137	396.3

A significant reduction in the size of elementary cell confirms our initial assumptions regarding the way of La^{3+} ions incorporate into the crystal lattice of BBN ceramics.

The temperature functions of the real part of dielectric permittivity (ε') is shown in Fig. 3. The maximum value of the presented dependences (ε'_{max}) decreases with an increase in dopant concentration. Moreover, all characteristics have a diffuse maximum, the temperature T_m of which is linearly dependent on the La content (Table 1 and inserted Fig. 2a). The same effect was visible in case of lanthanum modified SrBi$_2$Nb$_2$O$_9$ ceramics [28]. The diffuseness has been studied as a function of lanthanum content, by estimating the degree of diffuseness γ, using the following relation [29]:

$$\frac{1}{\varepsilon'} - \frac{1}{\varepsilon'_{max}} = \frac{(T - T_m)^\gamma}{C} \tag{1}$$

where ε_{max} is the maximum value of the dielectric constant at the transition temperature (T_m), C the Curie-like constant and γ is the
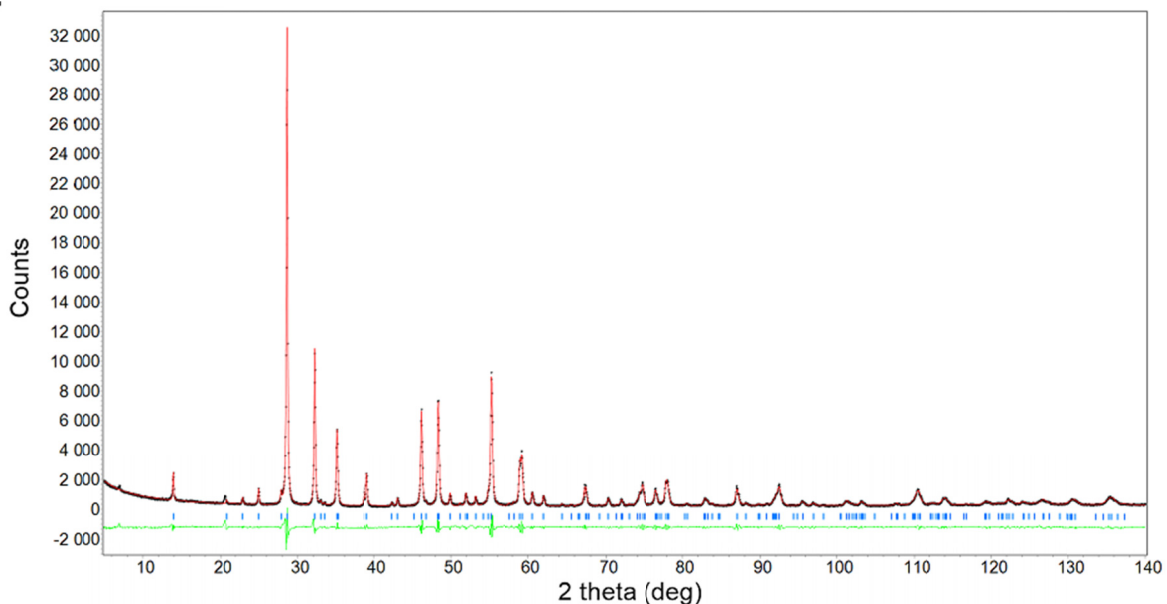

Fig. 2. X-ray diffraction pattern for BBN with lanthanum content 5at% refined with the Rietveld method
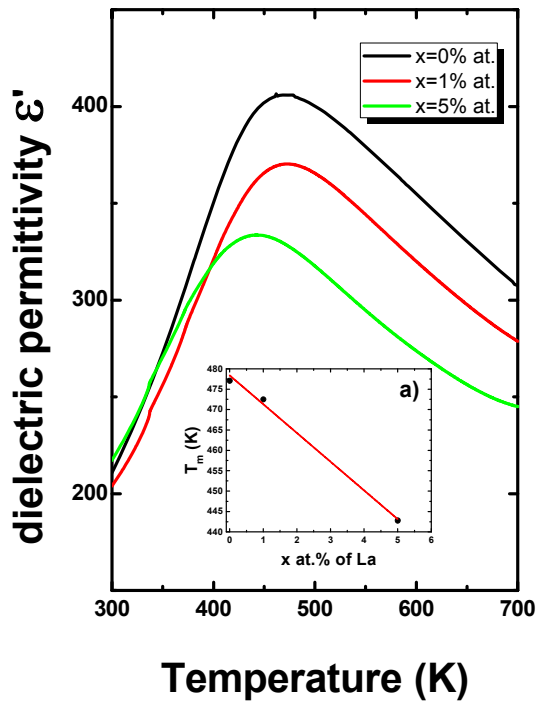
Fig. 3. The real part of dielectric permittivity as a function of the temperature, measured at frequency 10 kHz, for BBN ceramics with various La content, the T_m vs La content is shown in the inserted figure (a)

degree of diffuseness. The limiting values 1 and 2 for γ, respectively, reduce the expression to the Curie-Weiss law valid for a normal and the quadratic dependence valid for the ideal relaxor ferroelectric [30,31]. The values of γ factor for all investigated samples are collected in Table 2.

The pure $BaBi_2Nb_2O_9$ ceramics show strong frequency dependences of the maximum value of dielectric permittivity and the shifts of this maximum to high temperatures, with an increase of frequency. The lanthanum addition strengthens the effect of shift in temperatures and weakens the frequency dispersion of ε'_{max}, which is visible in Fig. 4 and Table 2.

The degree of dispersion of ε'_{max}, understood as $\Delta\varepsilon'_{max} = \varepsilon'_{max}(100\ Hz) - \varepsilon'_{max}(1\ MHz)$, decreases considerably from 121 for pure ceramics to 61 for ceramics with 5 at.% of lanthanum, whereas the degree of dispersion of T_m ($\Delta T_m = T_m(1\ MHz) - T_m(100\ Hz)$) increases from 93 K to 110 K.

TABLE 2

Temperatures T_m, ε_{max} determined from measurements of $\varepsilon(T)$ at $f = 100$ kHz, value of degree of diffusion γ, degree of ε'_{max} and T_m dispersion

x at. % La	T_m 100 kHz (K)	ε_{max} 100 kHz	g	ΔT_m (K)	$\Delta\varepsilon_{max}$
0	477.1	406	1.45	93	121
1	472.9	370	1.52	104	51
5	442.8	333	1.44	110	61

The results presented hereinabove do not allow to change the more likely way of lanthanum incorporation. The impedance spectroscopy should be a good tool for this purpose and give a clear answer.

Figure 5 shows a variation of the imaginary (Z_{re}) and real (Z_{im}) part of complex impedance as a function of frequency (10^2-10^6 Hz), at different temperature (623 K-823 K) for the lanthanum modified BBN ceramics. The dependences for pure BBN ceramics were presented in the previous paper [32].

It is observed that the value of Z_{re} decreases with rise in temperature and frequency (Fig. 5a), indicating an increase in AC conductivity with the rise in temperature as well as frequency [33]. Figure 5b shows the frequency and temperature dependence of loss spectrum $-Z_{im}$. The value of Z_{im} increased with increase in frequency and exhibited a maximum before starts decreasing rapidly. The broadening of the peak, which is slightly asymmetrical in nature, shifted towards higher frequencies as the temperature increases. A significant broadening of the peaks with an increase in temperature suggests that there is a spread of relaxation times, i.e., the existence of a temperature dependent electrical relaxation phenomenon in the material [34].
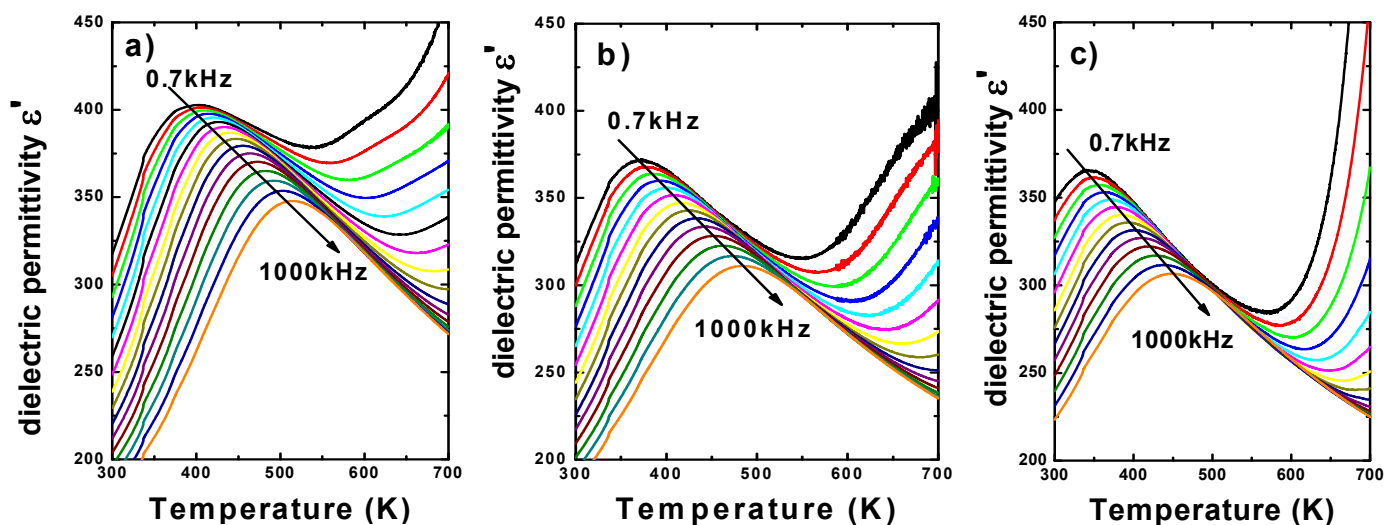

Fig. 4. Real part of dielectric permittivity as a function of temperature measured on heating at various frequencies of measuring field, for undoped BBN (a), BBN+1 at. %La (b) and BBN+5 at. %La (c) ceramics
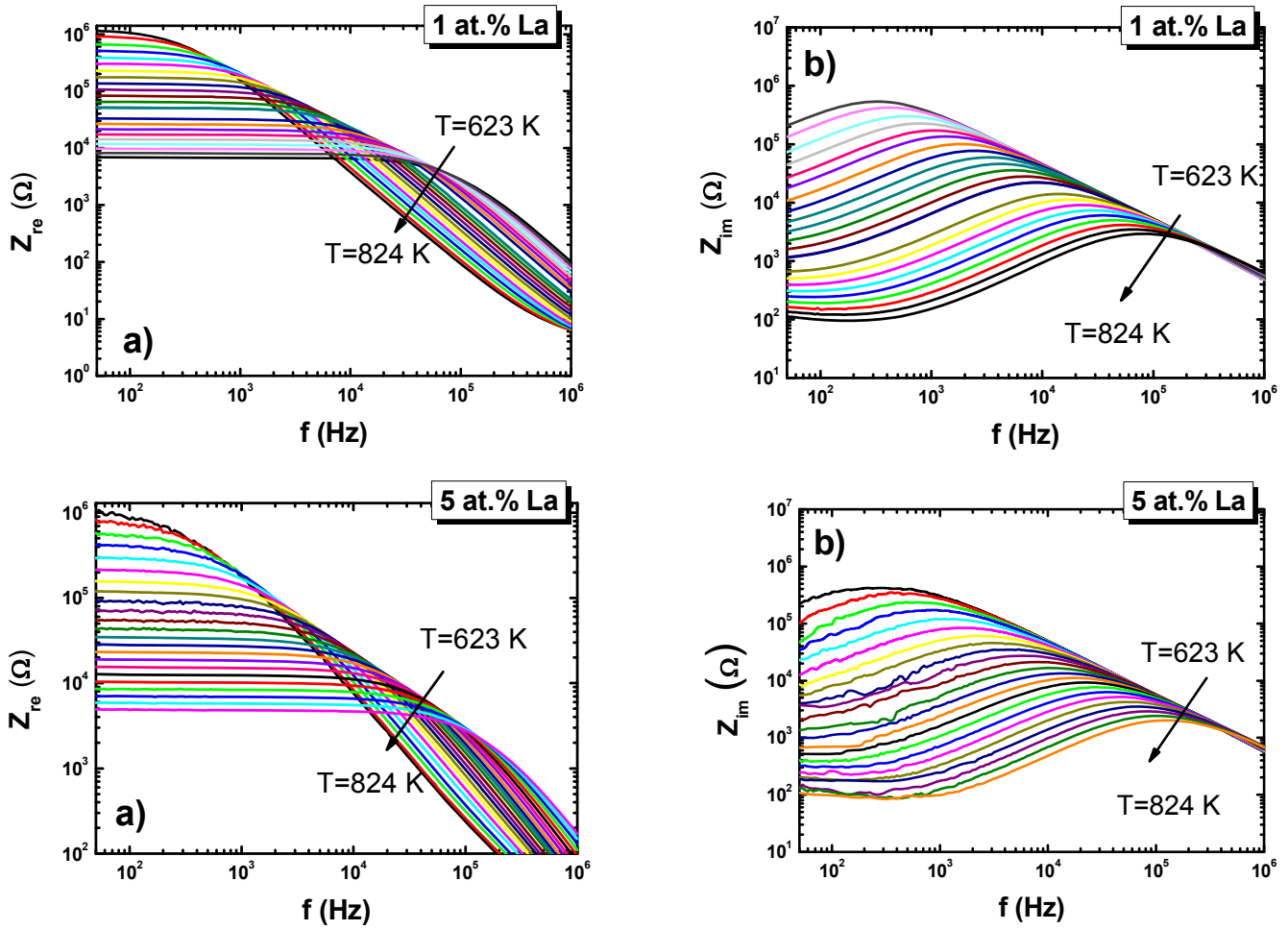
Fig. 5. The frequency dependence of real part (a)and imaginary (b) of the impedance at various temperature for BBN ceramics modified with lanthanum

The observed phenomenon may be a consequence of the presence of immobile species/electron at low temperature and defects/vacancies at higher temperature [35].

The first step of systematic procedure for the analysis of AC measurements is to plot the results in the complex impedance plane, Z_{re} vs Z_{im}. These plots are very useful for determining the equivalent circuit describing the electric properties of discussed ceramics materials. Figure 6 shows exemplary $Z_{re}(Z_{im})$ relations obtained for all samples at temperature 723 K.

The obtained curves are neither deformed semicircle nor circular arcs, the centre of which appears below the real axis. In the high frequency region, the Debye behaviour is observed – the angle between the tangent of the arc and the real axis is 90°. Whereas, in the part of arc where $f \rightarrow 0$ the angle is less than 90°. Such behaviour is prevalence for ceramics material characterized by perovskite structure [36] as well as ceramics belongs to the Aurivillius family [37-39]. Deviation from the classical semicircle entails the opportunity to correctly describe the electrical processes occurring in the sample, by means of a model of two overlapping semicircles. The semicircles, in high frequency regions, correspond to the grain electric properties, whereas the semicircles in low frequency regions describe the properties of grain boundary. After considering a series of
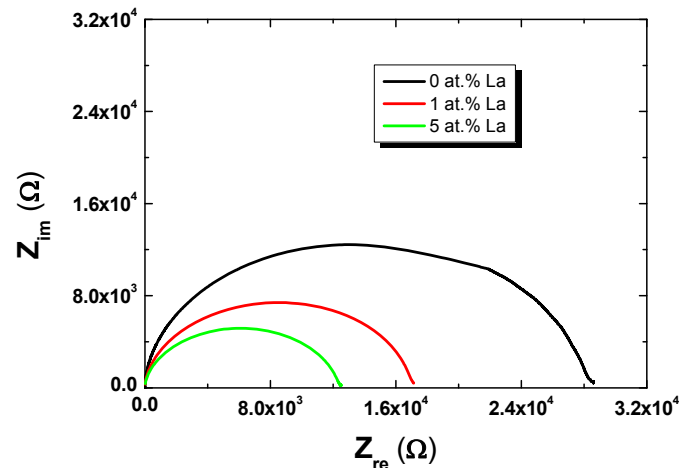

Fig. 6. Nyquist plot for BBN ceramics pure and La-doped obtained at temperature 723 K

literature reports, a circuit consisting of two branches in series, representing the properties of grain and grain boundary, were attributed to the obtained data for lanthanum modified BBN ceramics (Fig. 7). The equivalent circuit for pure BBN ceramics was a bit less complicated [32].
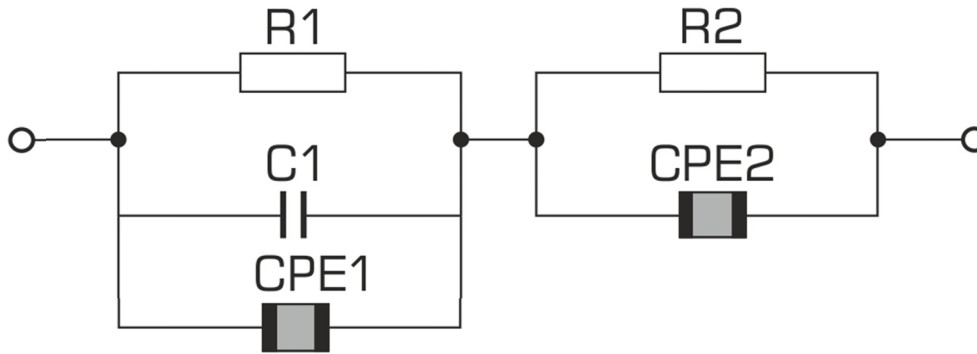
Fig. 7. Equivalent circuit used to represent the impedance response of BBN ceramics doped by lanthanum

The subsequent comprehensive analysis of measuring impedance data obtained for all discussed samples allowed to determinate the resistivity of grain (R_g) and grain boundary (R_{gb}). In case of pure BBN ceramics, the grain boundary resistivity was found to be much higher than the resistivity of grains. The tendency gradually changed with an increase in the

concentration of lanthanum dopant, namely the resistivity of grain boundaries significantly decreased, whereas the resistivity of grains increased. Exemplary values of the discussed resistivity for pure and modified samples determined at several selected temperatures are included in the Table 3.

The Arrhenius plot of grains and grains boundary resistivity has a linear character (Fig. 8), which signifies at the activation character of processes occurring in components of microstructure of investigated ceramics.

The slopes of $\ln R_g(1/T)$ dependences are not significantly different from each other, whereas the slopes of $\ln R_{gb}(1/T)$ changed drastically with the increase of lanthanum concentration. The activation energies for both grains and grains boundary resistivity were calculated from the slope of the discussed dependencies (Table 4).

Small differences in the energy values of grain activation and grain boundaries observed in pure and doped 1% lanthanum

TABLE 3

Resistivity of grains (R_g) and grain boundaries (R_{gb}) determined at several selected temperatures

x at.% La^{3+}	T [K]	R_g [Ω]	R_{gb} [Ω]
0	823	1613	9024
	773	4198	23338
	723	11907	66079
	673	40933	238670
	623	155330	818690
1	823	4064	2719
	773	9989	7315
	723	29336	28044
	673	128400	104520
	623	578170	395430
5	823	4127	604
	773	11482	1070
	723	41562	2283
	673	159590	7089
	623	839060	22938

TABLE 4

Activation energy values calculated from impedance data for grain (E_g) and grain boundary (E_{gb}) resistivity

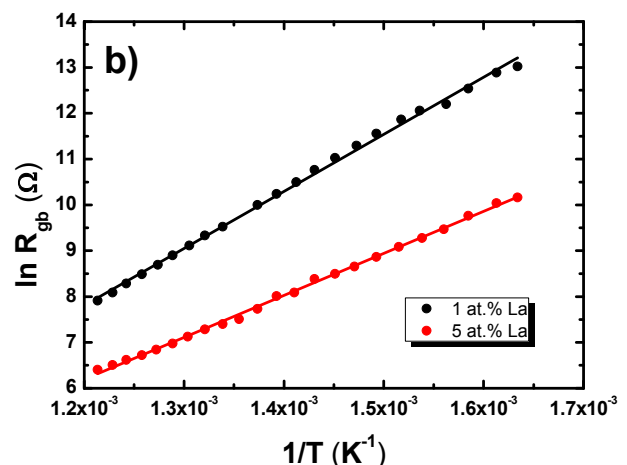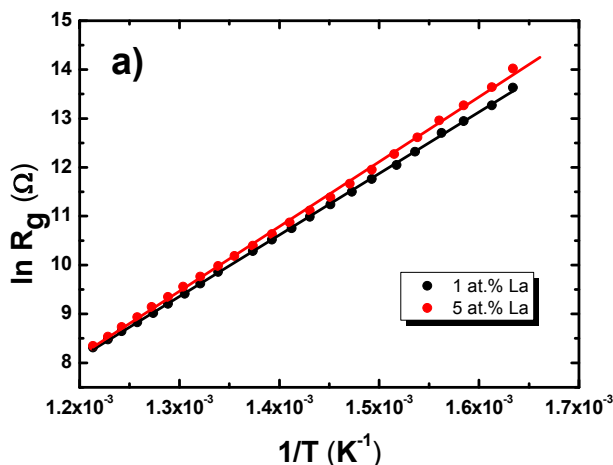| x at.% La^{3+}	E_g [eV]	E_{gb} [eV]
0	1	0.98
1	1.08	1.07
5	1.14	0.79

Fig. 8. Arrhenius plots for calculation of conduction activation energies of grain (a) and grain boundary (b)

ceramics suggest that the process of conductivity occurs to the same extent in grains, as well as in grains boundaries. The situation changes for the higher concentration of lanthanum – the activation energy of grains boundary is considerably smaller than the one of grains.

The significant changes in the value of the grains and grain boundaries resistivity indicated that the first scenario proposed in the introduction takes place. Namely, the trivalent lanthanum ions incorporate twovalent barium ions. In order to maintain the electric balance the creation of A-site cationic vacancies as well as the oxygen vacancies. Defects have the tendency to accumulate on the grain boundaries. The mechanism of conductivity in the Aurivillius family ceramics is mainly connected with the thermally activated oxygen vacancies [40]. The vacancies are the trapping centers for mobile charge carriers. At high temperatures, the charge carrier shopping among the oxygen vacancies. The increase in the number of oxygen vacancies facilitates electric carriers transporting, which is manifested by a significant reduction in the activation energy of conductivity. The increase in the activation energy of grains could be explained by the fact that the substitution of La^{3+} in the Ba^{2+} sites resulted in an enhanced stability of the perovskite structure a higher chemical bond strength associated with the La-O bonds than that of the Ba-O bonds. In addition, stronger chemical bonds would certainly suppress the formation of intrinsic defects and hamper the electric conductivity. In consequence, the energy needed to activate the process of conductivity increased [41].

4. Conclusions

The article reports the details of synthesis procedure, dielectric and electric properties of lanthanum modified $BaBi_2Nb_2O_9$ ceramics prepared by conventional mixed oxide and carbonates method. The lanthanum admixture causes an increase in the homogeneity of grain size and a significant reduction in the maximum value of dielectric permittivity. Moreover, the discussed modification is responsible for the subtle diminution of properties characteristic of ferroelectric relaxor. The lanthanum additive influences also on resistivity of grain and grain boundaries.

REFERENCES

[1] B. Aurivillius, Mixed bismuth oxides with layer lattices: I. The structure type $CaNb_2Bi_2O_9$, Arkiv For. Kemi (1), 463-480 (1949).

[2] B. Aurivillius, Mixed bismuth oxides with layer lattices: II. Structure of $Bi_4Ti_3O_{12}$, Arkiv For. Kemi (1), 499-512 (1949).

[3] B. Aurivillius, Mixed bismuth oxides with layer lattices: III. Structure of $BaBi_4Ti_4O_{15}$, Arkiv For. Kemi (2), 519-527 (1950).

[4] P. Millán, A. Castro, J.B. Torrance, The first doping of lead^{2+} into the bismuth oxide layers of the aurivillius oxides, MRS Bull. **28** (2), 117-122 (1993).

[5] A. Moure, Review and perspectives of Aurivillius structures as a lead-free Piezoelectric system, Appl. Sci. **8** (1), 62 2018.

[6] P. Millan, A. Ramirez, A. Castro, Substitutions of smaller Sb^{3+} and Sn^{2+}cations for Bi^{3+} in Aurivillius-like phases, J. Mater. Sci. **14**, 1657-1660 (1995).

[7] A. Castro, P. Millan, R. Enjalbert, Structural evolution of the Aurivillius framework in the solid solutions Bi_2WO_6-Sb_2WO_6, MRS Bull. **30** (7), 871-882 (1995).

[8] M. Dion, M. Ganne, Stabilite relative des types structuraux $Ca_2TlTa_5O_{15}$ et bronze quadratique de tungstene, MRS Bull. **15** (c), 121-128 (1980).

[9] L.E. Cross, Relaxor ferroelectrics, Ferroelectrics **76**, 241-267 (1997).

[10] A.A. Bokov, Z.G. Ye, Recent progress in relaxor ferroelectrics with perovskite structure, J. Mater. Sci. **41** (1), 31-52 (2006).

[11] V.V. Shvartsman, D.C. Lupascu, Lead-free relaxor ferroelectrics, J. Am. Ceram. Soc. **95** (1), 1-26 (2012).

[12] M. Adamczyk, L. Kozielski, R. Zachariasz, M. Pawełczyk, L. Szymczak, Structural, dielectric specroscopy and internal friction correlation in $BaBi_2Nb_2O_9$ ceramics, Arch. Metall. Mater. **59** (1), 40-43 (2014).

[13] Y. Shimakawa, Y. Kubo, Crystal structure and ferroelectric properties of $ABi_2Ta_2O_9$ (A=Ca, Sr, and Ba), Phys. Rev. **61** (10), 6559-6564 (2000).

[14] R. Macquart, B.J. Kennedy, T. Vogt, Ch.J. Howard, Phase transition in $BaBi_2Nb_2O_9$: Implications for layered ferroelectrics, Phys. Rev. **66**, 212102-1-212102-4 (2002).

[15] B.R. Kannan, B.H. Venkataraman, Dielectric relaxor and conductivity characteristics of undoped and samarium doped barium bismuth niobate ferroelectric ceramics, Ferroelectrics **43** (4-6), 82-89 (2015).

[16] M.K. Adak, A. Mukherjee, A. Chowdhury, U.K. Ghorai, D. Dhak, Structure-property correlation of $Ba_{1-x}Cu_xBi_2(Nb_{1-x}Ta_x)_2O_9$ ferroelectric nano ceramics prepared by chemical route, J. Alloys Compd. **740**, 203-211 (2018).

[17] M.X. Façanha, F.F. Carmo, J.P.C. Nascimento, T.O. Sales, W.Q. Santos, A.S. Gouveia-Neto, C.J. Silva, A.S.B. Sombra, A novel white-light emitting BaBi2Nb2O9: $Li^+/Tm^{3+}/Er^{3+}/Yb^{3+}$ upconversion phosphor, J. Lumin. **204**, 539-547 (2018).

[18] Y. Wu, Ch. Nguzen, S. Seraji, M. Forbess, S.J. Limmer, Processing and Properties of Strontium Bismuth Vanadate Ferroelectric Ceramics, J. Am. Ceram. Soc. **84**, 2882-2888 (2001).

[19] M. Adamczyk, L. Kozielski, M. Pilch, M. Pawełczyk, A. Soszyński, Influence of vanadium dopant on relaxor behavior of $BaBi_2Nb_2O_9$ ceramics, Ceram. Int. **39** (4), 4589-4595 (2013).

[20] C. Karthik, K.B.R. Varma, M. Maglione, J. Etourneau, Relaxor characteristics of layered $Ba_{1-(32)x}La_xBi_2Nb_2O_9$ Ceramics, J. Appl. Phys. **101** (1), 2-8 (2007).

[21] Y. Shimakawa, Y. Kubo, Y. Tauchi, H. Asano, T. Kamiyama, F. Izumi, Z. Hiroi, Crystal and electronic structures of $Bi_{4-x}La_xTi_3O_{12}$ ferroelectric materials, Appl. Phys. Lett. **79** (17), 2791-2793 (2001).

[22] J. Zhu, X.B. Chen, Z.P. Zhang, J.C. Shen, Raman and X-ray photoelectron scattering study of lanthanum-doped strontium bismuth titanate, Acta Mater. **53** (11), 3155-3162 (2005).

[23] B.A. Boukamp, A Linear Kronig-Kramers Transform Test for Immittance Data Validation, J. Electrochem. Soc. **142** (6), 1885-1894 (1995).

[24] B.A. Boukamp, Electrochemical impedance spectroscopy in solid state ionics: recent advances, Solid State Ion. **169** (1-4), 65-73 (2004).

[25] X.P. Jiang, X.J. Wang, J.X. Wen, C. Chen, N. Tu, X.H. Li, Microstructure and electrical properties of Mn-modified bismuth-layer $Na_{0.25}K_{0.25}Bi_{2.5}Nb_2O_9$ Ceramics, J. Alloys Compd. **544**, 125-128 (2012).

[26] C.M. Wang, J.F. Wang, L.M. Zheng, Enhancement of the piezoelectric properties of sodium lanthanum bismuth titanate ($Na_{0.5}La_{0.5}Bi_4Ti_4O_{15}$) through modification with cobalt, Mater. Sci. Eng. B **171**, 79-85 (2010).

[27] M. Adamczyk, Z. Ujma, M. Pawełczyk, Dielectric properties of $BaBi_2Nb_2O_9$ ceramics, J. Mater. Sci. **41**, 5317-5322 (2006).

[28] S.E. Park, J. Cho, T.K. Song, M.H. Kim, S.S. Kim, H.S. Lee, Ionic Doping Effects in $SrBi_2Nb_2O_9$ Ferroelectric Ceramics, J. Electroceramics **13** (1-3), 51-54 (2004).

[29] H.T. Martirena, J.C. Burfoot, Grain-size effects on properties of some ferroelectric ceramics, J. Phys. Condens. Matter. **7**, 3182-3192 (1974).

[30] D.C. Sinclair, T.B. Adams, F.D. Morrison, A.R. West, $CaCu_3Ti_4O_{12}$: One-step internal barrier layer capacitor, Appl. Phys. Lett. **80**, 2153-2155 (2002).

[31] J. Muscat, A. Wander, N.M. Harrison, On the prediction of band gaps from hybrid functional theory, Chem. Phys. Lett. **342**, 397-401 (2001).

[32] M. Adamczyk, L. Kozielski, M. Pilch, Impedance Spectroscopy of $BaBi_2Nb_2O_9$ Ceramics, Ferroelectrics **417**, 1-8 (2011).

[33] S. Selvasekarapandian, M. Vijaykumar, The ac impedance spectroscopy studies on $LiDyO_2$, Mater. Chem. Phys. **80**, 29-33 (2003).

[34] G. Goodman, R.C. Buchanan, T.G. Reynolds, Ceramic materials for electronics, Buchanan Marcel Dekker, New York, (1986).

[35] P. Dhak, D. Dhak, M. Das, K. Pramanik, P. Pramanik, Impedance spectroscopy study of LaMnO3 modified BaTiO3 ceramics, Mater. Sci. Eng. B **164**, 165-171 (2009).

[36] A. Peláiz-Barranco, I. González-Carmenate, F. Calderón-Piñar, E. Torres-García, AC behavior and PTCR effect in PZN-PT-BT ferroelectric ceramics, Solid State Commun. **132** (7), 431-435 (2004).

[37] B.H. Venkataraman, K.B.R. Varma, Impedance and dielectric studies of ferroelectric $SrBi_2Nb_2O_9$ ceramics, J. Phys. Chem. Solids. **64** (11), 2105-2112 (2003).

[38] L. Zhigao, J.P. Bonnet, J. Ravez, J.M. Rjzau, P. Hagenmuller, An impedance study of $Pb_2KNb_5O_{15}$ ferroelectric ceramics, J. Phys. Chem. Solids **53** (1), 1-9 (1991).

[39] J.S. Kim, J.N. Kim, Impedance Spectra near the Phase Transition Temperature of Potassium Lithium Niobate Crystals, Jpn. J. Appl. Phys. **39**, 3502-3505 (2000).

[40] S.K. Kim, M. Miyayama, H. Yanagida, Electrical anisotropy and a plausible explanation for dielectric anomaly of $Bi_4Ti_3O_{12}$ single crystal, MRS Bull. **31**, 121-131 (1996).

[41] S. Kumar, K.B.R. Varma, Influence of lanthanum doping on the dielectric, ferroelectric and relaxor behaviour of barium bismuth titanate ceramics, J. Phys. D **42** (7), 075405-075414 (2009).